*Free Radical Research*, January 2009; 43(1): 47–57

informa
healthcare

# Free radical generation in rosmarinic acid investigated by electron paramagnetic resonance spectroscopy

KATHARINA F. PIRKER[1], CHRISTOPHER W. M. KAY[2], KLAUS STOLZE[3], DANIEL TUNEGA[4,5], THOMAS G. REICHENAUER[1], & BERNARD A. GOODMAN[1,6]

[1]*Department of Environmental Research, Austrian Research Centers GmbH-ARC, Seibersdorf, Austria,* [2]*Institute of Structural & Molecular Biology and London Centre for Nanotechnology, University College London, London, UK,* [3]*Molecular Pharmacology and Toxicology Unit, Department for Biomedical Sciences, University of Veterinary Medicine Vienna, Vienna, Austria,* [4]*Institute for Theoretical Chemistry, University of Vienna, Vienna, Austria,* [5]*Institute of Soil Research, University of Natural Resources and Applied Life Sciences, Vienna, Austria, and* [6]*Department of Chemistry & Chemical Engineering, Guangxi University, Nanning, Guangxi, PR China*

Accepted by Professor M. Davies

*(Received 22 August 2008; revised 24 October 2008)*



**Abstract**
Free radical generation as a result of oxidation reactions of rosmarinic acid (RA), a caffeic acid ester with 3, 4-dihydroxyphenyllactate, was investigated by electron paramagnetic resonance (EPR) spectroscopy using a variety of oxidation conditions. Limitations and possibilities of using the various methodologies to obtain information about the reaction chemistry of polyphenols are discussed. Three different spectra were detected dependent on the pH and oxidizing agent. Feasible structures for the observed radicals were tested by density functional theory (DFT) calculations and the results indicate that oxidation reactions can occur at both of the catechol groups.

**Keywords:** *Rosmarinic acid, EPR spectroscopy, auto-oxidation, superoxide anion radical, free radical.*

## Introduction

In recent years, the chemical behaviour of polyphenols has attracted increasing attention as a result of the association of foods that are rich in polyphenols with positive health effects. This is commonly assigned to the high antioxidant activity of polyphenols, especially those in which catechol and/or pyrogallol groups are present in the molecules [1].

Although there are nutritionally important antioxidants which are regenerated after oxidation by a redox cycling process, e.g. $\alpha$-tocopherol, this is not necessarily the only type of reaction exhibited by phenolic compounds. For example, only spectra from degradation products of the flavonoid kaempferol could be detected by EPR spectroscopy after alkaline auto-oxidation [2,3], although this molecule has similar antioxidative properties to those of its isomer luteolin, which can redox cycle [4]. Nevertheless, the potential for redox cycling can be regarded as one important feature if a molecule is likely to function as a biological antioxidant by scavenging reactive oxygen species (ROS) and hence to protect cells from oxidative damage.

The present work describes the oxidative chemistry of the polyphenol rosmarinic acid (RA), a water-soluble ester of 3,4-dihydroxycinnamic acid and 3, 4-dihydroxyphenyllactate (Figure 1). RA is found mainly in the family of *Lamiaceae* [5], and can be

Correspondence: Katharina F. Pirker, Department of Environmental Research, Austrian Research Centers GmbH-ARC, A-2444 Seibersdorf, Austria. Tel: +43 50550 3577. Fax: +43 50550 3520. Email: katharina.pirker@arcs.ac.at

ISSN 1071-5762 print/ISSN 1029-2470 online 
DOI: 10.1080/10715760802585236

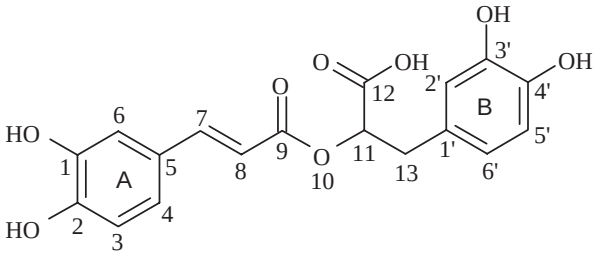


Figure 1. Structure of RA showing the convention for numbering the carbon atoms used in the present paper.

extracted from the herb rosemary, where it is stored in the vacuole of the plant cell.

The two catechol groups on rings A and B can be oxidized to o-quinones and are able to inactivate peptides by binding to them [6]. RA has been reported to have anti-viral, antibacterial, anti-tumour, anti-hepatitis, anti-mutagenic, anti-allergic, anti-carcinogenic and anti-inflammatory properties. It also inhibits HIV-1 and blood clotting [6–10].

There are a number of previous reports of electron paramagnetic resonance (EPR) measurements of free radical formation in RA by alkaline oxidation [5, 11–14] and by oxidation with HRP/$H_2O_2$ at pH 9.5 [7,15], but they contain considerable discrepancies in both the hyperfine coupling (hfc) constants and their assignments. Apart from the selection of spectral acquisition parameters, the main reason for differences between results is probably the choice of experimental conditions, e.g. pH, influence of $O_2$, solvent composition.

A reinvestigation of the oxidation of RA using EPR spectroscopy has now been performed, with the aim of improving our knowledge of its free radical chemistry and obtaining a better understanding of its antioxidant behaviour. The formation of 'stable' free radicals was investigated using five different oxidation conditions. RA was auto-oxidized at pH 13 and oxidized by a Fenton reaction system (i.e. the hydroxyl (·OH) radical), superoxide anion radicals ($O_2^{\bullet -}$), generated from potassium superoxide ($KO_2$), and ROS generated by two enzymatic systems at pH 7. Putative free radical structures obtained by interpretation of the EPR spectra were then tested using density functional theory (DFT) calculations.

## Materials and methods

The polyphenol rosmarinic acid (≥ 97% purity) and the enzyme horseradish peroxidase (HRP) were purchased from Fluka (Vienna, Austria), xanthine oxidase (XO) (from bovine milk, Grade III) and superoxide dismutase (SOD) (from bovine erythrocytes) were purchased from Sigma (Vienna, Austria), xanthine (X) from Merck (now VWR International GmbH, Vienna, Austria) and potassium superoxide from Aldrich (Vienna, Austria). Enzyme activities were: HRP: ~ 150 units/mg; XO: ~ 29 units/ml (one unit converts 1.0 μmole of X to uric acid per min at pH 7.5 at 25°C; ~ 50% of the activity is obtained with hypoxanthine as substrate); SOD: 2500–7000 units/mg.

### *Auto-oxidation procedures*

The influence of oxygen was investigated by two different experimental setups, as reported by Pirker et al. [3]. In the first procedure ('auto-oxidation at solution interface') 0.1 M NaOH and 1 mM RA (dissolved in DMSO) were added consecutively to an EPR flat cell (Wilmad-Labglass, Buena, NJ). The auto-oxidation reaction occurred at the interface of the two solutions and involved dissolved oxygen as the oxidizing agent. In the second procedure ('auto-oxidation in mixed solutions') the two solutions were mixed in air in a microfuge tube and the resulting mixture was then transferred to an EPR flat cell. In this latter procedure, the effects of different volume ratios of 1 mM RA and 0.1 M NaOH (1:1, 1.67:1 and 3:1) were also investigated. In a modification of this latter method, RA was also auto-oxidized using a pump flow system in which 1 mM RA (in $H_2O$) and 0.1 M NaOH solutions were mixed at the bottom of a flat cell already located in the spectrometer cavity. By subsequently stopping the pump, the kinetics of the degradation of Radical 1 and the development of Radical 2 were investigated.

### *Oxidation with horseradish peroxidase/hydrogen peroxide (HRP/$H_2O_2$)*

Oxidation with the system HRP/$H_2O_2$ used solutions with concentrations similar to those of Miura et al. [16]. The oxidizing solution consisted of 200 μl of a potassium phosphate buffer (50 mM, pH 7), which were mixed in a microfuge tube with 50 μl of $ZnCl_2$ (10 mM), 50 μl HRP (12.5 μM) and 5 μl $H_2O_2$ (100 μM). All solutions were made with Millipore water (Millipore, Simplicity 185, Vienna, Austria). The mixed solution (200 μl) was transferred into an EPR flat cell and 200 μl of 1 mM RA (dissolved in DMSO) were then added.

Generation of ·OH radicals was confirmed in the presence and absence of RA by the spin trapping method using dimethyl-1-pyrroline-*N*-oxide (DMPO) as spin trap. This was investigated by first mixing 150 μl phosphate buffer (50 mM, pH 7), 50 μl $ZnCl_2$ (10 mM), 50 μl HRP (12.5 μM), 200 μl DMPO (50 mM) and 50 μl $H_2O$ (with 4.8% DMSO) or 50 μl of 10 mM RA (in $H_2O$ with 4.8% DMSO) and then initiating radical production by adding 5 μl $H_2O_2$.

### *Oxidation with xanthine/xanthine oxidase (X/XO)*

The system X/XO was used to generate $O_2^{\bullet -}$. The experiment was carried out in 200 μl of potassium

phosphate buffer (50 mM, pH 7), which was mixed for a few seconds with 20 µl of X solution (657 µM) and 5 µl of XO solution (8 µl XO/1 ml $H_2O$; ~0.23 units/ml reaction solution). All individual solutions were prepared with Millipore water. The final solution mixture (200 µl) was transferred to an EPR flat cell and 200 µl of 1 mM RA (dissolved in DMSO) were then added.

Generation of $O_2^{\cdot -}$ radicals was investigated in the presence and absence of RA by the spin trapping method using DMPO as spin trap. This was tested by first mixing 250 µl X (1 mM in a 50 mM phosphate buffer, pH 7), 190 µl DMPO (50 mM) and 50 µl $H_2O$ (with 4.8% DMSO) or 50 µl RA (10 mM in $H_2O$ with 4.8% DMSO) and then starting the reaction by adding 10 µl XO solution (10 µl XO/1 ml $H_2O$).

*Oxidation in a Fenton reaction system*

·OH radicals are generated in the Fenton system as a result of the reaction of $H_2O_2$ with Fe(II). The reagent concentrations used were those of Blank et al. [17], except that ascorbic acid was omitted in the present work. Millipore water was used for preparation of the individual solutions. A mixture of 200 µl of potassium phosphate buffer (50 mM, pH 7) with 5 µl $FeCl_3 \times 6H_2O$ (10 mM), 5 µl EDTA (25 mM) and 5 µl $H_2O_2$ (100 µM) were placed in a microfuge tube and the solution was mixed for a few seconds using a Vortex mixer. The mixed solution (200 µl) was transferred to a flat cell and 200 µl of 1 mM RA (in DMSO) were then added. The flat cell was placed in the spectrometer within 1 min of the solutions being prepared and EPR spectra were recorded immediately after tuning the spectrometer.

The spin trap DMPO was used to investigate the generation of ·OH radicals in the presence and absence of RA. A solution of 235 µl potassium phosphate buffer (50 mM, pH 7), 5 µl $FeCl_3 \cdot 6H_2O$ (10 mM), 5 µl EDTA (25 mM), 200 µl DMPO (50 mM) and 50 µl of $H_2O$ (with 4.8% DMSO) or 50 µl RA (10 mM in $H_2O$ with 4.8% DMSO) were mixed and the reaction initiated by adding 5 µl $H_2O_2$.

*Oxidation with potassium superoxide*

The reaction of RA with $O_2^{\cdot -}$ radicals was also investigated using $KO_2$ as the oxidizing agent in a non-aqueous system. A 50 mM $KO_2$ solution in DMSO was prepared according to Valentine et al. [18]. The $KO_2$-solution (200 µl) was mixed with 200 µl of 10 mM RA (dissolved in DMSO) solution in a microfuge tube. The resulting solution was then transferred to an EPR flat cell which was placed in the spectrometer and the spectrum was recorded as quickly as possible (~1 min after mixing the solutions).

*EPR spectroscopy*

All EPR spectra were acquired in 1024 points using either a Bruker ESP 300E CW spectrometer equipped with an ER4103TM cavity or a Bruker EMX CW spectrometer equipped with a high sensitivity resonator, both operating at X-band frequencies. Microwave generation was by a klystron in the ESP 300E and a Gunn diode in the EMX spectrometer and in both spectrometers the microwave frequency was recorded continuously using an inline frequency counter. For most of the spectra a modulation frequency (MF) of 100 kHz was chosen. The microwave power (MP) and modulation amplitude (MA) used for recording the various spectra are indicated in the relevant figure captions.

After placing the flat cell in the microwave cavity, the spectrometer was tuned manually to minimize the time between commencement of the reaction and recording the spectrum.

All of the parameters derived from the spectra were refined by simulation using the Bruker Simfonia software and *g*-values are expressed relative to diphenylpicrylhydrazyl (DPPH) ($g = 2.0036$), which was used as an external standard.

*DFT calculations*

DFT calculations were performed with the GAUSSIAN® 03 program [19]. The ground states of the RA molecule in the free radical oxidized forms were optimized at the unrestricted B3LYP/6-31G level of the theory. Then the hfc constants were calculated using the same B3LYP functional and the EPR-II basis set on the B3LYP/6-31G geometry.

## Results and interpretation

*Auto-oxidation*

Auto-oxidation of RA at the interface of the two reaction solutions gave EPR spectra with two radical components, a 19 peak spectrum (Radical 1, Figure 2A) which was stable for ~5 min., followed by a 14 peak spectrum (Radical 2, Figure 2B). The spectrum of Radical 1 was simulated with five $^1H$ couplings, whereas the spectrum of Radical 2 was simulated with four inequivalent $^1Hs$. The hfc constants and g-values of all detected radicals are given in Table I.

When the reaction solutions were mixed prior to being transferred to the flat cell, auto-oxidation of RA always produced the 14 peak spectrum (Radical 2), irrespective of the RA:NaOH volume ratio, although there were slight differences in the hfc constants (Table I). With the highest level of RA (RA:NaOH ratio of 3:1), a weak 19 peak spectrum (Radical 1) was detected initially, but this was quickly replaced by the 14 peak spectrum of Radical 2, whereas Radical 2

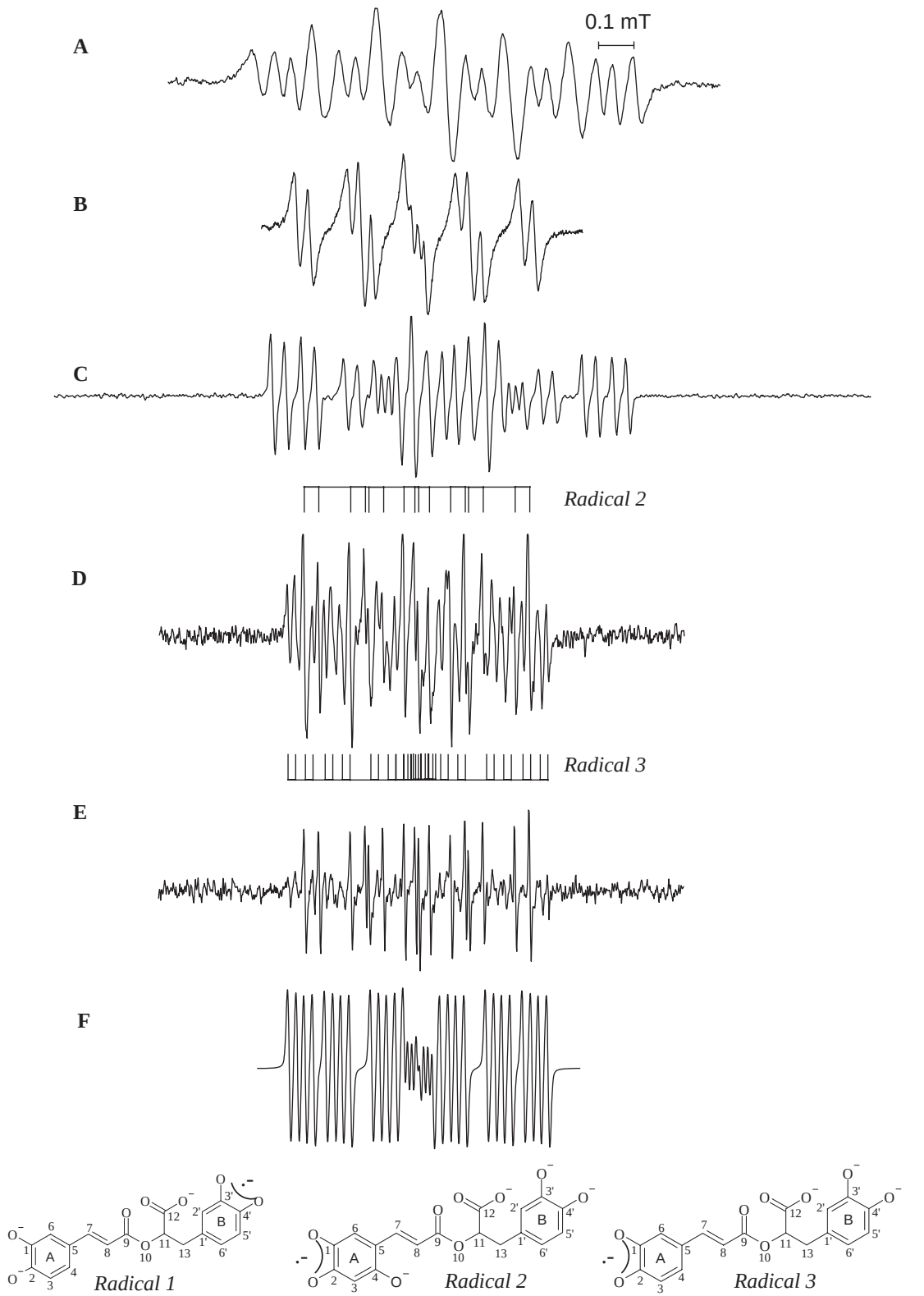


Figure 2. EPR spectra of Radicals 1, 2 and 3 from alkaline auto-oxidized RA at the interface of the reaction solutions (A, B) and using the flow-system (C–E). (A) Radical 1 (MA 0.01 mT, MP 20 mW) and (B) Radical 2 (MA 0.001 mT, MP 20 mW), (C) Radical 1 (pump on; MA 0.01 mT, MP 2 mW), (D) Radical 2 and 3 (pump off; MA 0.01 mT, MP 2 mW), (E) Radical 2 (pump off; MA 0.002 mT, MP 2 mW), (F) simulation of Radical 3.

was the only radical observed from the outset with lower RA:NaOH ratios.

Because of the indication in the above experiments that the initial free radical is short-lived, RA auto-oxidation was also investigated using a stop-flow system. The initial radical was similar to Radical 1 (Figure 2C), although there were slight differences in the hfc constants from those seen in the previous

Table I. Variation with experimental conditions of the hfc constants (mT) in the spectra from RA oxidation.

| | Oxidation type | a($^1$H) | a($^1$H) | a($^1$H) | a($^1$H) | a($^1$H) | g-values |
|---|---|---|---|---|---|---|---|
| Radical 1 | Auto-oxidation at solution interface Enzymatic systems (50% DMSO) | 0.360 | 0.360 | 0.178 | 0.108 | 0.059 | 2.0047 |
| | Flow system (100% $H_2O$) | 0.367 | 0.323 | 0.212 | 0.087 | 0.039 | 2.0046 |
| | $O_2^{\cdot-}$ (100% DMSO) | 0.357 | 0.329 | 0.220 | 0.150 | 0.102 | 2.0050 |
| Radical 2 | Auto-oxidation at solution interface | 0.305 | 0.178 | 0.145 | 0.038 | | 2.0044 |
| | Auto-oxidation in mixed solutions (RA:NaOH = 1:1) | 0.302 | 0.176 | 0.146 | 0.037 | | |
| | Auto-oxidation in mixed solutions (RA:NaOH = 1.67:1) | 0.307 | 0.176 | 0.146 | 0.036 | | |
| | Auto-oxidation in mixed solutions (RA:NaOH = 3:1) | 0.318 | 0.175 | 0.151 | 0.034 | | |
| | Flow system (stopped, 100% $H_2O$) | 0.286 | 0.184 | 0.133 | 0.042 | | 2.0045 |
| Radical 3 | Flow system (stopped, 100% $H_2O$) | 0.329 | 0.236 | 0.105 | 0.046 | 0.024 | 2.0044 |
| | $O_2^{\cdot-}$ (100% DMSO) | 0.292 | 0.207 | 0.160 | 0.106 | 0.106 | 2.0050 |
| | Enzymatic systems (50% DMSO) | 0.257 | 0.235 | 0.114 | 0.110 | 0.107 | 2.0047 |

measurements, probably because of the different solvent conditions (100% water) that were used. After the pump was switched off, the signal from Radical 1 disappeared quickly and was replaced by a spectrum (Figure 2D) which consists of at least two components. One of these corresponds to Radical 3, which was detected for $\sim$10 min after the pump was switched off and could be simulated with five inequivalent hfc constants (Table I). The other radical component (Radical 2, Figure 2E) was stable for $>$ 3 h.

### *Oxidation with $O_2^{\cdot-}$ and $^{\bullet}OH$ radicals*

Oxidation of RA by $O_2^{\cdot-}$ (generated by $KO_2$) resulted in a spectrum containing two components (Figure 3A), whose simulations are shown in Figure 3B and C. They are similar to Radicals 1 and 3 from the auto-oxidation experiments (Table I), except that the hydroxyl groups are protonated in the 100% DMSO solution (Figure 3, bottom), but deprotonated in alkaline conditions (Figure 2, bottom). Radical 1 was unstable, but Radical 3 could be detected for $>$ 16 h. The differences in hfc constants are probably the consequence of using different solvents (100% DMSO in the $O_2^{\cdot-}$ experiment, but 0–50% DMSO in the auto-oxidation experiment).

Similar spectra were obtained when RA was oxidized by the Fenton reaction system and the enzymatic systems HRP/$H_2O_2$ and X/XO at pH 7, provided the oxidant and the substrate were transferred into the flat cell consecutively. All generated spectra consisted of at least two components with similar stabilities (Figure 4A–C), one of which was Radical 1. The spectra obtained using the Fenton reaction and HRP/$H_2O_2$ (Figure 4A and B) had to be recorded with higher modulation amplitude than that using X/XO, because of low signal intensities. Consequently, the spectrum obtained using X/XO as oxidizing agent (Figure 4C) shows better resolution. When the spectrum of Radical 1 (Figure 2A) was subtracted from Figure 4C, the remaining spectral intensity (Figure 4D) corresponded to Radical 3 (Figure 3C, Table I).

### *Interpretation*

All assignments of hfc constants are based on DFT calculations of the electron distribution in the proposed radicals after structure optimization. A comparison of the DFT results with the experimental hfc constants for all radicals is given in Table II.

Radical 1 most likely corresponds to oxidation of ring B (Figure 5A). Similar hfc constants were published by Pedersen [5] and Mouhajir et al. [12] for alkali oxidized RA. At pH 10, Maegawa et al. [11] obtained a similar radical to Radical 1, but with two more hfc constants of $<$ 0.1 mT. They interpreted the EPR spectrum as corresponding to two simultaneously generated monophenolate radicals on the two oxygens of ring B. Bors et al. [15] also investigated the oxidation of RA by HRP/$H_2O_2$ at alkaline pH of 9.5 and assigned the spectrum to B-ring oxidation. A structure based on B-ring oxidation is also supported by the similarity of the magnitudes of the hfc constants to those of oxidized dihydrocaffeic acid (Figure 5B) [20]. According to the DFT calculations, the two largest hfc constants arise from interaction of the unpaired electron with one of the two $^1$H atoms in position 13 and with the $^1$H in position 6'. The other coupling constants can be assigned to the $^1$H on C 11 and the $^1$Hs in position 5' and 2'.

Radical 2 was only observed in alkaline solutions, where it was much more stable than Radical 1. Following the DFT calculation of Cao et al. [8], it is likely that this radical is derived from oxidation at the A-ring. However, the spectrum was simulated with four $^1$Hs, whereas oxidation of the A-ring would be expected to lead to five $^1$H coupling constants (taking into account the $^1$Hs on the double bond in the $\alpha$- and $\beta$-position to the aromatic ring). It is possible that carbon 4 becomes hydroxylated to give the radical shown in Figure 5C, in an equivalent

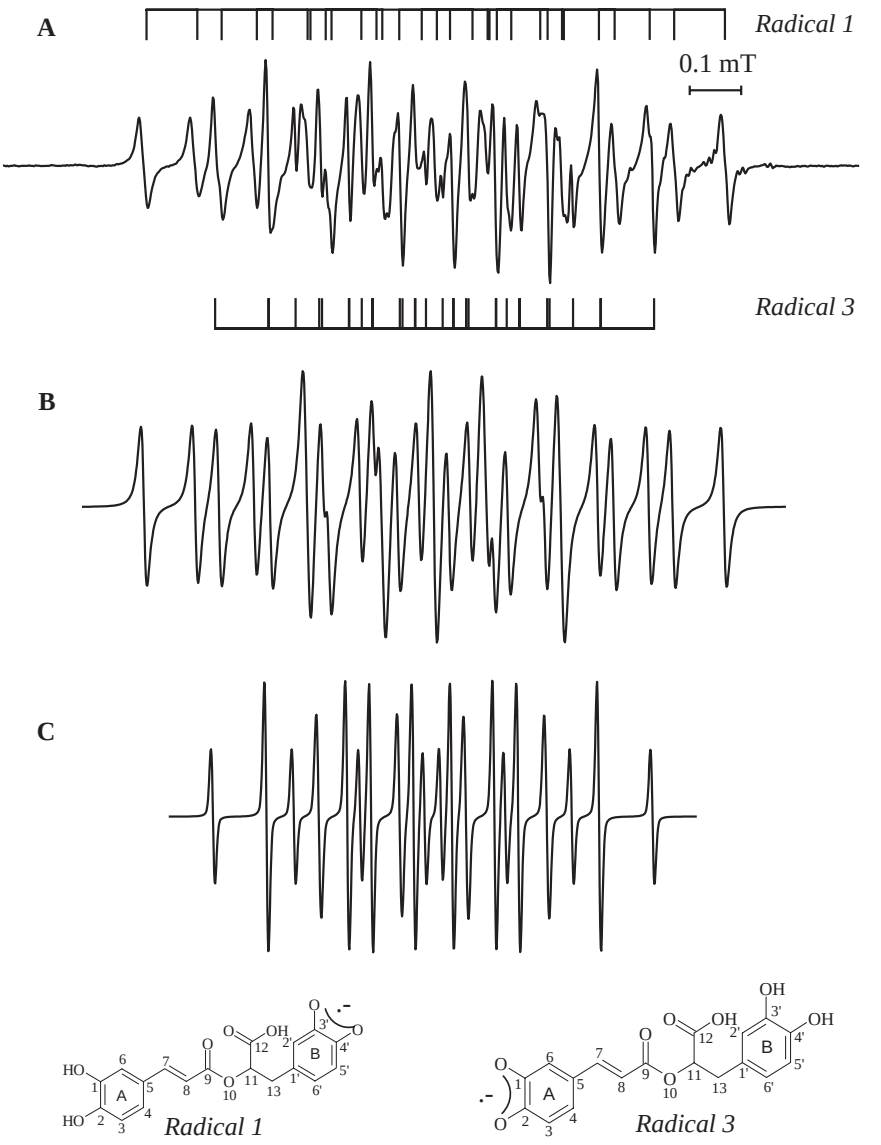


Figure 3. EPR spectra of RA oxidized by $O_2^{\cdot -}$. (A) Radical 1 and Radical 3 (MA 0.001 mT, MF 10 kHz, MP 0.2 mW), (B) simulation of Radical 1, (C) simulation of Radical 3.

reaction to that reported by Ashworth [21] for the formation of trihydroxycinnamic acids by hydroxylation of dihydroxycinnamic acids during prolonged auto-oxidation in strongly alkaline solution. The hfc constants are in fairly good agreement with those of Pedersen and Ollgaard [20] and Ashworth [21] for the radical from 2,4,5-trihydroxycinnamic acid (Figure 5D). The assignments in Table II are based on the DFT calculations and the largest hfc constant arises from the $^1H$ in position 8.

Radical 3 was detected together with Radical 1 at pH 7 and after oxidation by $O_2^{\cdot -}$ radicals; it was also an intermediate radical product during alkaline auto-oxidation using the stopped flow system. It is likely that it corresponds to the radical formed by oxidation on ring A, as predicted by Cao et al. [8]. Further support for this interpretation is obtained by comparison of the hfc constants with those reported for oxidized 3,4-dihydroxycinnamic acid in alkaline and acidic media [7,21,22] and those of oxidized chlorogenic acid [5,20]. The hfc constants of this radical show a high sensitivity to solvent composition (Table I), the biggest difference being apparent between 100% $H_2O$ (alkaline auto-oxidation, flow system) and 100% DMSO (oxidised by $O_2^{\cdot -}$). A proposed structure for Radical 3 is shown in Figure 5E, together with the structure of 3,4-dihydroxycinnamic acid as the model compound (Figure 5F). The assignements of the hfc constants given in Table II are based on results of the DFT calculations. Petrucci et al. [14] have also proposed that a radical formed from RA during alkaline oxidation by $PbO_2$ corresponds to the oxidation product of ring A. However, the hfc constants of their radical (0.334, 0.320, 0.190, 0.128, 0.083 mT) are in closer agreement with those of Radical 1, where oxidation occurs

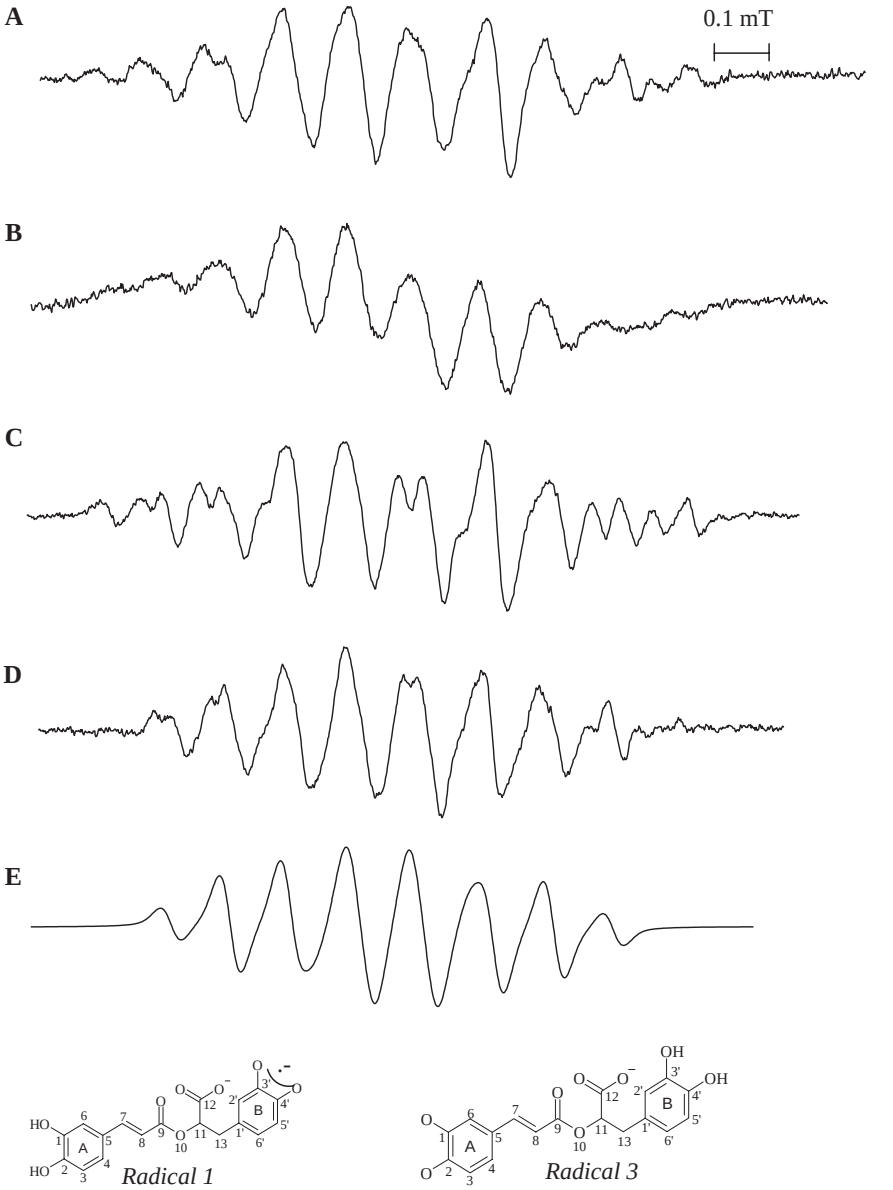


Figure 4. EPR spectra of RA oxidized by (A) Fenton reaction system (MA 0.03 mT), (B) HRP/$H_2O_2$ (MA 0.05 mT), (C) X/XO (MA 0.01 mT), (D) residual spectrum after subtraction of Radical 1 from spectrum (C), (E) simulation of (D) using the parameters for Radical 3 in Table I (20 mW MP).

on ring B (Table I). The RA radical obtained by Bors et al. [7] after oxidation by HRP/$H_2O_2$ at pH 9 was also interpreted as corresponding to the oxidized A-ring, although the two smallest hfc constants were absent from their EPR spectrum.

The generation of $^{\bullet}OH$ and $O_2^{\bullet -}$ radicals was confirmed in the experiments at pH 7 using the spin trap DMPO, which is sensitive to oxygen-centred radicals. Interestingly, RA functioned differently in the three radical generating systems. In the Fenton reaction system (with no ascorbic acid), in which iron was provided as Fe(III), $^{\bullet}OH$ radical generation occurred only in the presence of RA. Thus we presume that RA reduced Fe(III) to Fe(II) and was oxidized itself. A typical spectrum from the Fenton reaction mixture in the presence of DMPO and RA is shown in Figure 6A. It consists of three DMPO-adduct signals, the $^{\bullet}OH$-adduct, the $O_2^{\bullet -}$-adduct and a C-centred radical adduct. Under these experimental conditions where RA was added before the reaction started, a very weak EPR signal was detected in the absence of the spin trap, indicating the build up of only low concentrations of a radical by RA oxidation.

$^{\bullet}OH$ radical generation was confirmed in the system HRP/$H_2O_2$ in both the absence and presence of RA. When RA was added before the reaction started, a triplet signal (0.23, 0.16 mT) was detected together with the $^{\bullet}OH$-DMPO-adduct (Figure 6B). Since this triplet was also detected in the absence of the spin trap, but not in the absence of RA, it probably arises from oxidized RA, but it was not possible to assign it to a specific radical.

Table II. Comparison of experimental hfc constants with those obtained from DFT calculations.

| | | | | | | |
|---|---|---|---|---|---|---|
| Radical 1 | $a_2$, | $a_5$, | $a_6$, | $a_{13(CH2)}$ | $a_{11}$ | |
| Experiment (flow system) | 0.087 | 0.212 | 0.323 | 0.367 | 0.039 | |
| DFT | 0.132 | 0.214 | 0.287 | 0.344 | 0.022 | |
| Radical 2 | $a_3$ | $a_6$ | $a_7$ | $a_8$ | | |
| Experiment (auto-oxidation at solution interface) | 0.038 | 0.178 | 0.145 | 0.305 | | |
| DFT | 0.031 | 0.289 | 0.045 | 0.369 | | |
| Radical 3 | $a_3$ | $a_4$ | $a_6$ | $a_7$ | $a_8$ | $a_{11}$ |
| Experiment (flow system, stopped) | 0.046 | 0.105 | 0.329 | | 0.236 | 0.024 |
| Experiment ($O_2^{\bullet -}$) | 0.106 | 0.160 | 0.292 | | 0.207 | 0.106 |
| DFT | 0.171 | 0.215 | 0.367 | | 0.233 | 0.012 |

The system X/XO generated $O_2^{\bullet -}$ radicals which could be trapped by DMPO (Figure 6C), but within a few minutes the spectrum of the $O_2^{\bullet -}$-DMPO adduct was replaced by that of the $^{\bullet}$OH-DMPO-adduct due to a rearrangement of the radical adduct [23]. No EPR signal was observed when RA was present in the reaction solution, presumably because of inhibition of XO which has been shown previously for RA [24].

Thus it was necessary to transfer the X/XO reaction solution and the RA solution (in DMSO) consecutively to the flat cell, so that a sufficient $O_2^{\bullet -}$ radical concentration could be built up before reaction with RA. The relatively slow mixing of the $H_2O$ and DMSO phases allows the $O_2^{\bullet -}$ scavenging reaction to be observed before radical generation ceases as a result of enzyme inhibition by RA.

## Discussion

Three radical species were detected after oxidizing RA under alkaline or neutral conditions and these results indicate that radical formation can occur on either of the two catechol groups (rings A and B), as suggested previously by DFT calculations [8]. Although ring B is a stronger electron donor than ring A, the radical formed on ring A is more stable. Based on these facts and on published hfc constants for *o*-semiquinone radicals substituted in *p*-positions, it was possible to assign structures for the observed radicals, which were then tested by our own DFT calculations. The results strongly suggest that Radical 1 in the present work is formed by oxidation of the catechol group in ring B, whereas Radicals 2 and 3 are generated by oxidation of ring A.

The radicals reported by Maegawa et al. [11], Mouhajir et al. [12] and Pedersen [5,13], are similar to Radical 1, but none of the present spectra agree with the results of Bors et al. [7,15]. However, we were able to reproduce the results from Bors et al. [7,15] when measurements were repeated using their experimental setup. There is ambiguity in the spectral assignments of Bors et al. [7,15], the hfc constants being assigned to an oxidized B-ring in one experiment [15], but to an oxidized A-ring in the other [7]. Petrucci et al. [14] assigned the radical they observed on RA oxidation to the oxidized A-ring, but the hfc constants are closer to the radical we assign to B-ring oxidation. Especially at alkaline pH, where the semiquinone structure is based on a dianion, it is very likely that the spin density of the unpaired electron is delocalized over $O_3$ and $O_4$. Bors et al. [7,15] suggested the simultaneous formation of $O_3$- and $O_4$-semiquinones but, in the absence of any chelating agent, only the $O_4$-semiquinone was assumed to be stable enough to be detected by EPR. Zn (II) is a known and common chelating agent to stabilize diphenolate radicals. It was used as a component in the HRP/$H_2O_2$ oxidation procedure, but in experiments with the X/XO system the addition of Zn(II) decreased the signal intensity of the RA radicals dramatically (data not shown). This is likely to result from inhibition of the enzyme XO by Zn(II) [25], with a final concentration of 2 mM in the reaction solution. Maegawa et al. [11] also interpreted their RA radical as corresponding to the presence of two separate monophenolate forms of the B-ring. In the present measurements, the magnitudes of the hfc constants determined by DFT calculations are consistent with the radical anion, where the unpaired electron is delocalized over both O-atoms, being formed at pH 13 and 7, as well as for $O_2^{\bullet -}$ oxidation in DMSO.

The good agreement with reported hfc constants from oxidized 2,4,5-trihydroxycinnamic acid [20,21] strongly suggests that Radical 2 is hydroxylated at carbon 4 under the strong alkaline conditions that we used. Furthermore, there is good agreement between the $^1$H coupling constants for Radical 3 and those from 3,4-dihydroxycinnamic acid [21], which has a similar structure to the A-ring part of the RA structure, and with those from chlorogenic acid [5,20]. Radical 3 showed a strong solvent dependency of the hfc constants and this could be a reason for differences between experimental and calculated hfc constants, especially for the small values.

The radicals derived from RA oxidation in enzymatic systems at pH 7 were strongly influenced by the order of mixing the reagents. In the case of X/XO, radical generation was only seen when the oxidizing solution (in $H_2O$) and the RA solution (in DMSO) were added consecutively to the flat cell, presumably because of inhibition of the enzyme by RA. With

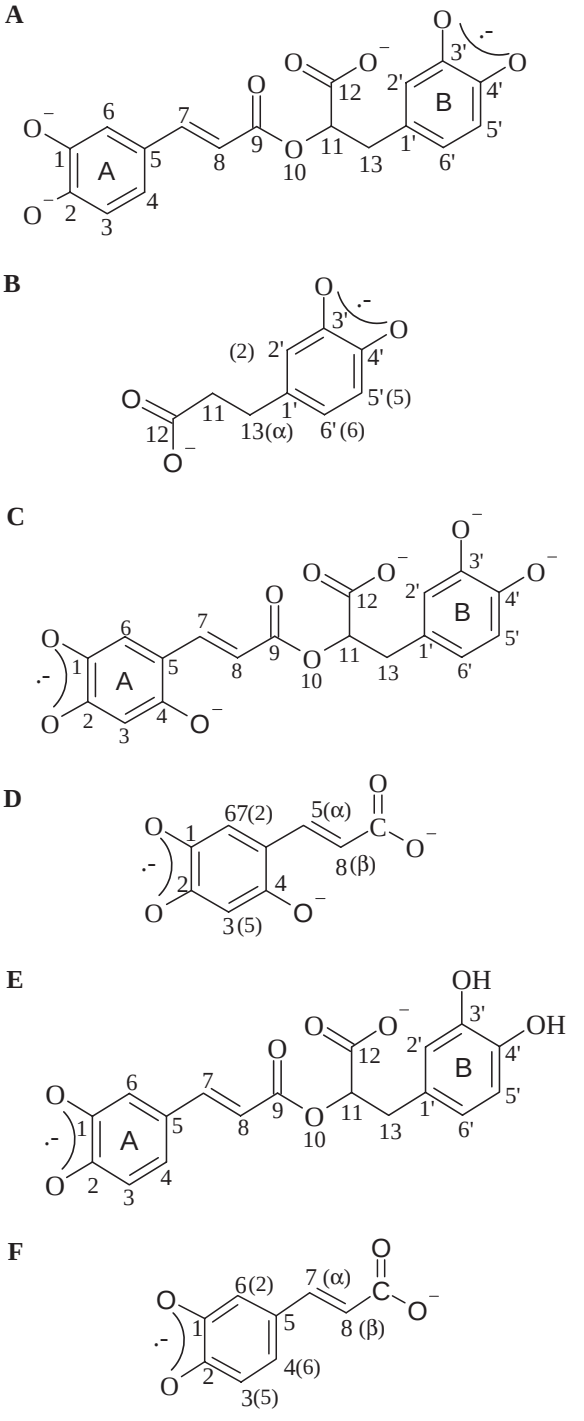


Figure 5. Proposed structures for (A) Radical 1 from RA, (B) the radical from dihydrocaffeic acid [20], (C) Radical 2 from RA, (D) the radical from 6-hydroxycaffeic acid [20], (E) Radical 3 from RA and (F) the radical from 3,4-dihydroxycinnamic acid [21]. The numbering of the model compounds (B, D, F) has been adapted to that in Figure 1, numbers according to the conventional nomenclature for these structures are in brackets.

$HRP/H_2O_2$ the presence of RA had little effect on $^{\bullet}OH$ radical generation, but the spectrum from oxidized RA, when RA was in the initial solution, was different (a triplet) from that obtained when RA was added later (Radical 1 and 3). This suggests an interaction of RA with HRP, as described by Jakopitsch et al. [26], where the antioxidant serves as a hydrogen donor between different oxidation states of the enzyme. With the Fenton reaction system, RA was active in $^{\bullet}OH$ radical generation and $O_2^{\bullet -}$ radicals and a C-centred radical were also detected in spin trapping experiments. Nevertheless, the RA radical signal was very weak in solutions in which RA was present from the beginning of the reaction. It seems that RA acts as a reducing agent for the Fe(III) on the one hand, but on the other hand it also scavenges ROS.

Oxidation of both rings was detected in all experiments, but differences were detected in the stability of the radicals. At alkaline pH, using the flow-system, the signal from Radical 1 was the only one observed when the pump was on. Once the pump was switched off, this signal was immediately replaced by the spectra of Radical 2 and 3. At pH 7, Radicals 1 and 3 were both formed and had similar stabilities in the enzymatic and Fenton reaction systems. On the other hand, when RA was oxidized by $O_2^{\bullet -}$ in pure DMSO, Radical 1 was less stable, although Radicals 1 and 3 were initially formed to similar extents.

According to Cao et al. [8] the bond dissociation energies (BDE) of the protons of the hydroxyl groups on carbon 2 (ring A) and 4' (ring B) are similar and low, which makes hydrogen abstraction likely to occur from either ring. In addition, ring B has the highest electron density in the highest occupied molecular orbital (HOMO) in the ground state molecule, indicating that this is the part of the molecule with the best electron donation properties. However, the lowest unoccupied molecular orbital (LUMO) is located mainly on ring A, which consequently has the better electron delocalization properties and forms a more stable radical. This argument supports the observed stability of Radicals 2 and 3, in which ring A is oxidized, and the short half-life of Radical 1 at alkaline pH and in DMSO, where the B-ring is oxidized. The simultaneous appearance of Radicals 1 and 3 at neutral pH after oxidation by $HRP/H_2O_2$, X/XO and the Fenton reaction could be an effect of either a continuous oxidation of ring B or an interaction between rings A and B. The possibility of the formation of a biradical in RA was tested at low temperature (77 K). No peaks were observed that could correspond to electron–electron dipole interactions. Furthermore, hfc constants from DFT calculations of triplet state electron configurations for doubly oxidized RA deviated from experimentally obtained hfc constants (data not shown).

The observation of hydroxylation in ring A after alkaline auto-oxidation at the interface of the two reaction solutions suggests an earlier oxidation of ring A which was not visible in the EPR spectra. An explanation could be a fast reaction rate of the oxidized A-ring with hydroxyl ions under such strong

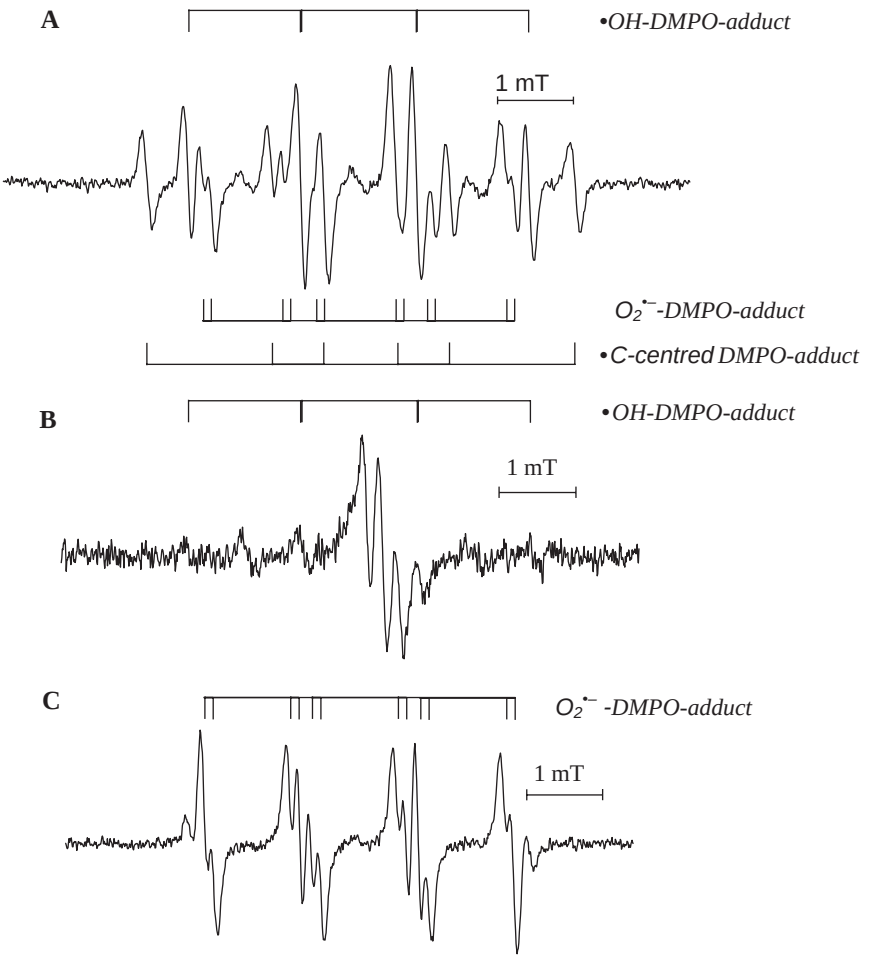


Figure 6. EPR spectrum of (A) the Fenton reaction system in the presence of RA (MA 0.1 mT), (B) HRP/$H_2O_2$ system in the presence of RA (MA 0.1 mT), (C) the X/XO system (MA 0.1 mT) using DMPO as spin trap (20 mW MP).

alkaline conditions. This is also a reasonable explanation for the EPR-spectra seen on alkaline oxidation, where the RA stock solution and NaOH were mixed with $O_2$ in a tube before being transferred to the EPR flat cell. In those experiments the hydroxylated component (Radical 2) was visible from the beginning of the EPR measurements.

## Conclusions

The results of this work give further insight into the free radical chemistry of the polyphenolic ester RA. Contrary to previous reports based on EPR studies, the present work shows that both rings A and B can be oxidized, but the stability of the resulting radicals varies with experimental conditions. The basic structure of the molecule was maintained in all of the radicals observed in the present experiments, suggesting that these oxidation products could be reduced under appropriate conditions. Although the EPR technique provides no information on diamagnetic products that might result from further oxidation of RA, the relative stability of the radicals, especially at physiological pH values, indicates that they could form a redox-cycling system, an important property for a biological antioxidant molecule.

By relating the EPR measurements to results from DFT calculations of the electronic structure of putative radical species, it was possible to assign the various hfc constants to $^1H$ atoms in the radicals with greater confidence than previously and some changes in previously published assignments have been proposed.

## Acknowledgements

This work was funded by the Austrian Ministry of Traffic, Innovation and Technology (BMVIT) and the Austrian Science Fund (FWF). We thank the University College London for access to the central computing cluster. We are also grateful for technical support and the computer time at the Linux-PC cluster Schrödinger III of the Computer Center of the University of Vienna.

***Declaration of interest*:** The authors report no conflicts of interest. The authors alone are responsible for the content and writing of the paper.

## References


[1] Rice-Evans CA, Miller NJ, Paganga G. Structure-antioxidant activity relationships of flavonoids and phenolic acids. Free Radic Biol Med 1996;20:933–956.

[2] Miller E, Schreier P. Studies on flavonol degradation by peroxidase (donor: H2O2-oxidoreductase, EC 1.11.1.7): Part 1-Kaempferol. Food Chem 1985;17:143–154.

[3] Pirker KF, Stolze K, Reichenauer TG, Nohl H, Goodman BA. Are the biological properties of kaempferol determined by its oxidation products? Free Radic Res 2006;40:513–521.

[4] Cotelle N, Bernier J-L, Catteau J-P, Pommery J, Wallet J-C, Gaydou EM. Antioxidant properties of hydroxy-flavones. Free Radic Biol Med 1996;20:35–43.

[5] Pedersen JA. Distribution and taxonomic implications of some phenolics in the family Lamiaceae determined by ESR spectroscopy. Biochem Syst Ecol 2000;28:229–253.

[6] Berger A. Versuche zur Klonierung der Rosmarinsäuresynthase und anderer Gene der Rosmarinsäure-Biosynthese aus *Coleus blumei* [dissertation]. Düsseldorf (D): Heinrich-Heine-Universität; 2001.

[7] Bors W, Michel C, Stettmaier K, Lu Y, Foo LY. Antioxidant mechanisms of polyphenolic caffeic acid oligomers, constituents of *Salvia officinalis*. Biol Res 2004;37:301–311.

[8] Cao H, Cheng W-X, Li C, Pan X-L, Xie X-G, Lie T-H. DFT study on the antioxidant activity of rosmarinic acid. J Mol Struc-Theochem 2005;719:177–183.

[9] Milić BL, Milić NB. Protective effects of spice plants on mutagenesis. Phytother Res 1998;12:S3–S6.

[10] Ito H, Miyazaki T, Ono M, Sakurai H. Antiallergic activities of rabdosiin and its related compounds: chemical and biochemical evaluations. Bioorgan Med Chem 1998;6:1051–1056.

[11] Maegawa Y, Sugino K, Sakurai H. Identification of free radical species derived from caffeic acid and related polyphenols. Free Radic Res 2007;41:110–119.

[12] Mouhajir F, Pedersen JA, Rejdali M, Towers GHN. Phenolics in Moroccan medicinal plant species as studied by electron spin resonance spectroscopy. Pharm Biol 2001;39:391–398.

[13] Pedersen JA. Naturally occurring quinols and quinones studied as semiquinones by electron spin resonance. Phytochemistry 1978;17:775–778.

[14] Petrucci R, Astolfi P, Greci L, Firuzi O, Saso L, Marrosu G. A spectroelectrochemical and chemical study on oxidation of hydroxycinnamic acids in aprotic medium. Electrochim Acta 2007;52:2461–2470.

[15] Bors W, Michel C, Stettmaier K, Lu Y, Foo LY. Pulse radiolysis, electron paramagnetic resonance spectroscopy and theoretical calculations of caffeic acid oligomer radicals. Biochim Biophys Acta 2003;1620:97–107.

[16] Miura T, Muraoka S, Fujimoto Y. Inactivation of creatine kinase induced by quercetin with horseradish peroxidase and hydrogen peroxidase: pro-oxidative and anti-oxidative actions of quercetin. Food Chem Toxicol 2003;41:759–765.

[17] Blank I, Pascual EC, Devaud S, Fay LB, Stadler RH, Yeretzian C, Goodman BA. Degradation of the coffee flavor compound furfuryl mercaptan in model *Fenton*-type reaction systems. J Agr Food Chem 2002;50:2356–2364.

[18] Valentine JS, Miksztal AR, Sawyer DT. Methods for the study of superoxide chemistry in nonaqueous solutions. Methods Enzymol 1984;105:71–81.

[19] Frisch MJ, Trucks GW, Schlegel HB, Scuseria GE, Robb MA, Cheeseman Jr, Montgomery JA JR, Vreven T, Kudin KN, Burant JC, Millam JM, Iyengar SS, Tomasi J, Barone V, Mennucci B, Cossi M, Scalmani G, Rega N, Petersson GA, Nakatsuji H, Hada M, Ehara M, Toyota K, Fukuda R, Hasegawa J, Ishida M, Nakajima T, Honda Y, Kitao O, Nakai H, Klene M, Li X, Knox JE, Hratchian HP, Cross JB, Adamo C, Jaramillo J, Gomperts R, Stratmann RE, Yazyev O, Austin AJ, Cammi R, Pomelli R, Ochterski JW, Ayala PY, Morokuma K, Voth GA, Salvador P, Dannenberg JJ, Zakrzewski VG, Dapprich S, Daniels AD, Strain MC, Farkas O, Malick DK, Rabuck AD, Raghavachari K, Foresman JB, Ortiz JV, Cui Q, Baboul AG, Clifford S, Cioslowski J, Stefenov BB, Liu G, Liashenko A, Piskorz P, Komaromi I, Martin RL, Fox DJ, Keith T, Al-Laham MA, Peng CY, Nanayakkara A, Challacombe M, Gill PMW, Johnson B, Chen W, Wong MW, Gonzalez C, Pople JA. Gaussian 03, Revision C.02. Wallingford, CT: Gaussian, Inc; 2004.

[20] Pedersen JA, Ollgaard B. Phenolic acids in the genus *Lycopodium*. Biochem Syst Ecol 1982;10:3–9.

[21] Ashworth P. Electron spin resonance studies of structure and conformation in anion radicals formed during the autoxidation of hydroxylated coumarins. J Org Chem 1976;41:2920–2927.

[22] Dixon WT, Moghimi M, Murphy D. Electron spin resonance study of the stereochemistry of radicals related to cinnamic acid. J Chem Soc Perk T 2 1975;1189–1191.

[23] Buettner GR, Oberley LW. Considerations in the spin trapping of superoxide and hydroxyl radical in aqueous systems using 5,5-dimethyl-1-pyrroline-1-oxide. Biochem Biophys Res Co 1978;83:69–74.

[24] Masuoka N, Isobe T, Kubo I. Antioxidants from *Rabdosia japonica*. Phytother Res 2006;20:206–213.

[25] Mondal MS, Mitra S. The inhibition of bovine xanthine oxidase activity by $Hg^{2}+$ and other metal ions. J Inorg Biochem 1996;62:271–279.

[26] Jakopitsch C, Wanasinghe A, Jantschko W, Furtmüller PG, Obinger C. Kinetics of interconversion of ferrous enzymes, compound II and compound III, of wild-type Synechocystis catalase-peroxidase and Y249F. J Biol Chem 2005;280:9037–9042.


This paper was first published online on iFirst on 16 December 2008.